ACS APPLIED MATERIALS & INTERFACES

Research Article

www.acsami.org

Graphene Oxide-Supported Ag Nanoplates as LSPR Tunable and Reproducible Substrates for SERS Applications with Optimized Sensitivity

Hui Hou,[†,‡] Ping Wang,[†] Jie Zhang,[†,‡] Chuanping Li,[†,‡] and Yongdong Jin*[,†]

[†]State Key Laboratory of Electroanalytical Chemistry, Changchun Institute of Applied Chemistry, Chinese Academy of Sciences, Changchun 130022, Jilin, P. R. China

[‡]University of Chinese Academy of Sciences, Beijing 100049, P. R. China

Supporting Information

ABSTRACT: Nanoparticles and nanohybrids with well-defined structures, along with tunable localized surface plasmon resonance (LSPR) properties and optimized sensitivity, are crucial and highly desired for surface-enhanced Raman spectroscopy (SERS) applications. In this article, we report on a very promising and flexible SERS platforms with a tunable LSPR response and sensitivity based on Ag nanoplates and graphene oxide (GO). The SERS detection sensitivity can be easily optimized and significantly improved by fine-tuning the LSPR band of the Ag nanoplate/GO substrates (to enhance the SERS response) during sample preparation. We applied the as-prepared SERS platform for sensitive SERS detection of 4-mercaptobenzoic acid and 4-aminothiophenol and found that the SERS signal varied markedly (by ∼10−15-fold) with the fine-tuning of the LSPR band. The SERS enhancement factor of the Ag nanoplate/GO complexes was more than 10^4 times larger than that obtained using spherical Ag nanoparticles. The as-prepared Ag nanoplate/GO platforms, because of their excellent stability and tunable LSPR properties, will find promising practical SERS applications.

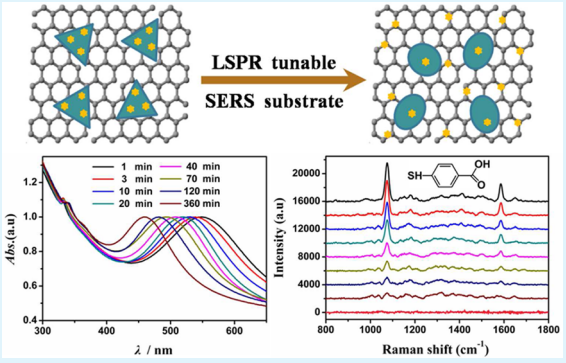

KEYWORDS: *graphene oxide, Ag nanoplates, localized surface plasmon resonance, surface-enhanced Raman spectroscopy, reproducibility, sensitivity*

1. INTRODUCTION

Raman spectroscopy is a very powerful surface trace analysis technique for the characterization of material structures and the detection of various analytes. Raman signals can be greatly enhanced if the target molecules modify or are adsorbed on properly prepared roughened (nanostructured) surfaces of metal substrates—a phenomenon discovered in the mid-1970s and called surface-enhanced Raman scattering (SERS).[1,2] In the past few decades, with the invention of various SERS-active nanostructured substrates, such as plasmonic Au, Ag, Cu, and transition metals, Raman spectroscopy studies and applications have aroused renewed interest recently.[3−6] Vigorous research activities have been carried out not only in air but also in electrochemical environments including a variety of metal surface morphologies, such as thin and thick films coated on roughened and smooth substrates, atomically smooth surfaces, powders, colloids, and even catalysts supported on insulator granules.[7−14] It has been found that the SERS effect differs in a number of ways from ordinary Raman spectroscopy and even from unenhanced surface Raman spectroscopy. More importantly, this effect makes it possible for SERS to be used as an in situ diagnostic method for determining the orientation of surface species and detailed molecular structures, which has been widely used in biological, electrochemical, and other areas.[15−22]

To extend the applications of SERS, the construction of highly active and stable SERS substrates is one of the most challenging steps to produce the desired signal enhancement. Among the noble metals, Ag nanomaterials are widely used and studied as SERS-active substrate because of their broad plasmon resonance in the visible region, high signal enhancement, and easy preparation compared with traditional metallic materials.[10,23−26] It is generally accepted that the SERS effect of molecules adsorbed on a roughened metal surface is induced by a combination of two mechanisms: (a) a chemical enhancement (CE) mechanism (with an enhancement factor of ∼10^2−10^4) and (b) an electromagnetic enhancement (EE) mechanism (with an enhancement factor of ∼10^6−10^8).[27,28] For most noble-metal systems, the EE mechanism, involving the surface morphology (shape and size) and corresponding localized surface plasmon resonance (LSPR) properties of the substrate, plays a dominant role in the SERS effect. To exploit the EE

Received: June 5, 2015
Accepted: July 23, 2015
Published: July 23, 2015

DOI: 10.1021/acsami.5b04946
ACS Appl. Mater. Interfaces 2015, 7, 18038−18045

mechanism for SERS applications, many approaches have been explored to prepare nanostructured Ag substrates, such as the silver mirror reaction for silver particle film,[29] aqueous-phase synthesis of silver nanoparticles,[30] electrochemical deposition of silver,[31] sulfide-mediated polyol method for Ag nanowires,[24] wet-chemical reduction for Ag dendrites,[32] laser ablation of Ag colloids,[33] and a self-assembly method for Ag nanoparticles (AgNPs).[34]

In this work, we report on a hybrid LSPR-tunable SERS substrate obtained by the controlled deposition of (SERS-active) Ag nanoplates on graphene oxide (GO) nanosheets,[35] as graphene has recently been shown to be another good SERS substrate.[36] The SERS detection sensitivity of the Ag nanoplate/GO substrate can be easily optimized and significantly improved by fine-tuning the LSPR band of the Ag nanoplate/GO substrate (to enhance the SERS response) during sample preparation. We applied this substrate successfully for the sensitive SERS detection of 4-mercaptobenzoic acid and 4-aminothiophenol and found that the SERS signal varied markedly (~10−15-fold) by just fine-tuning of the LSPR band. In addition, the as-prepared SERS substrate displayed high stability at room temperature over a long time (about several months), as reported in our previous work.[35] We believe that this facilely synthesized Ag nanoplate/GO platform will be promising for SERS-based biological and chemical detections.

2. EXPERIMENTAL SECTION

2.1. Materials. Sodium borohydride ($NaBH_4$, ≥99%), silver nitrate ($AgNO_3$), ascorbic acid (AA), poly(vinylpyrrolidone) (PVP; average Mw ≈ 29000), and 4-mercaptobenzoic acid (4-MBA) were purchased from Sigma-Aldrich. Trisodium citrate (TSC, ≥99%) was purchased from Sigma-Aldrich Fine Chemicals. Sodium nitrate ($NaNO_3$) was obtained from Xilong Chemical Industry Incorporated Co., Ltd. 4-Aminothiophenol (4-ATP) was purchased from J&K Scientific Ltd. Graphite powder was obtained from Alfa Aesar. Hydrogen peroxide (H_2O_2, 30 wt %), potassium permanganate ($KMnO_4$), and sulfuric acid (H_2SO_4) were purchased from Beijing Chemical Works. All of the chemicals were used as received without any further purification. Before the nanoparticle synthesis protocols, all stir bars and glassware were cleaned carefully in aqua regia [3:1 v/v HCl (37%):HNO_3 (65%)] solutions and then rinsed thoroughly with deionized water (DI water) before use. (*Caution: Aqua regia solutions are extremely corrosive and should be handled with extreme care, gloves and eye protection are required for handling. Never store these solutions in closed containers.*) All aqueous solutions were prepared using DI water. The DI water was prepared in a three-stage Millipore Milli-Q purification system and had a resistivity higher than 18.2 MΩ cm.

2.2. Synthesis of GO. GO was prepared from natural graphite powder using the modified Hummers method.[37] Briefly, GO was prepared by first mixing 1 g of graphite powder and 1 g of $NaNO_3$ in a clean flask; then, 45 mL of concentrated H_2SO_4 was added, and the solution was stirred vigorously for 10 min in an ice−water bath as a safety measure. While vigorous agitation was maintained, 1 g of $KMnO_4$ was slowly added to the suspension; then, the ice−water bath was removed, and the solution was transferred to a ~35 °C oil bath and stirred for about 1h. After that, 80 mL of DI water was slowly added into the solution under magnetic stirring for 30 min, causing an increase in temperature to ~98 °C during this process. Then, 200 mL of DI water and 6 mL of H_2O_2 (30%) were slowly added, and the color of the solution soon turned from dark brown to yellow. Finally, to remove the acid, the warm product was washed and filtered with a large amount of DI water. The dry form of GO was obtained by several cycles of centrifugation to remove all of the water-soluble byproducts and dried in a vacuum. To obtain a GO sheet solution, dry GO powder was dispersed in DI water (0.5 mg mL^{-1}) and then ultrasonicated for about 30 min under ambient conditions to obtain a clear solution. This aqueous GO solution was centrifuged at 30000 rpm for 15 min and further washed with DI water three times to remove any possible trace amount of impurities, which can affect the shape transformation of Ag nanoplates. Finally, the GO was dispersed in DI water at a concentration of 1.25 mg mL^{-1} for further use.

2.3. Synthesis of Ag Nanoplates. Ag nanoplates were synthesized according to the reported protocol.[38,39] First, 24.15 mL of DI water was combined with $AgNO_3$ (0.05 M, 50 μL), TSC (75 mM, 0.5 mL), H_2O_2 (30 wt %, 60 μL), and PVP (17.5 mM, 0.1 mL) sequentially under vigorous stirring at room temperature. Next, freshly made $NaBH_4$ (100 mM, 0.25 mL) (in ice-cold water) was injected into this mixture, which immediately generated a light-yellow solution, which was maintained for about 30 min. Then, the color of the colloidal suspension continued to change to dark yellow and quickly turned red, green, and blue within several seconds. To remove the byproducts, the unreacted reagents, and excess amounts of TSC and PVP, the obtained Ag nanoplates were centrifuged at 16000 rpm for 15 min and then washed twice with DI water. The resulting Ag nanoplates were then redispersed in 25 mL of DI water to keep the same concentration as the stock solution.

2.4. Complexing Ag Nanoplates with GO. To prepare Ag nanoplate/GO nanocomplexes, 22 mL of freshly prepared Ag nanoplate solution was simply mixed with 1 mL of purified GO aqueous solution under vigorous stirring at room temperature. Then, to obtain Ag nanoplate/GO complex suspensions with varying LSPR peak wavelengths, 1 mL of the mixture solution was removed at given time intervals, and a certain volume of TSC (75 mM, 0.3 mL) was added immediately to freeze the Ag nanoplate shape transformation (and hence their LSPR band). With the protection of sufficient citrate ions, the as-prepared Ag nanoplate/GO complexes exhibited excellent stability for a long time without any obvious changes in their optical properties.

2.5. Synthesis of AgNPs. AgNPs are synthesized according to the reported method.[40] To synthesize AgNPs with diameters of 50−60 nm, 0.125 mL of $AgNO_3$ (0.2 M) aqueous solution was rapidly added to 50 mL water under vigorous stirring. After this solution had been heated to a boil, 3 mL of TSC (1%) aqueous solution was quickly added, followed by 2 mL of 0.1 M AA solution. A quick color change from yellow to gray-yellow was observed upon the addition of AA. After being heated for 5−10 min, the solution was cooled under ambient conditions for characterization.

2.6. Instruments. Transmission electron microscopy (TEM) measurement was carried out by using a FEI TECNAI F20 EM instrument equipped with an energy-dispersive spectrometer at an accelerating voltage of 200 kV. TEM samples were prepared by placing a droplet of the final product on a carbon-coated copper grid and then allowing the sample to dry under ambient conditions. UV−vis−NIR absorption spectra were recorded using a Lambda 750 spectrometer (Perkin-Elmer, Wellesley, MA). X-ray photoelectron spectroscopy (XPS) measurements were recorded on a Thermo VG Scientific ESCALAB 250 spectrometer equipped with monochromatized Al Kα excitation. Raman spectra were collected through a Renishaw 2000 model confocal microscopy Raman spectrometer with a holographic notch filter and a CCD detector (Renishaw Ltd., Gloucestershire, U.K.) at ambient conditions, using the radiation at 514.5 nm from an air-cooled argon ion laser to excite the Raman absorption. The data acquisition time was 30 s with a power density of 20 mW for one accumulation. The Raman band of a silicon wafer at 520 cm^{-1} was used to calibrate the spectrometer. An Optotrace RamTracer-200 spectrometer with the radiation of a 785-nm laser was also used to collect Raman spectra. In this case, the data acquisition time was 5 s with a power density of 50 mW for one accumulation. The Raman bands of acetonitrile at 378, 918, and 1374 cm^{-1} were used to calibrate the spectrometer. All of the samples were suspended in water and put into a glass capillary for Raman measurements.

3. RESULTS AND DISCUSSION

3.1. Preparation and LSPR Property of the Ag Nanoplate/GO Complex. Triangular Ag nanoplates were

DOI: 10.1021/acsami.5b04946
ACS Appl. Mater. Interfaces 2015, 7, 18038−18045

prepared according to the reported method (see Experimental Section).[38,39] As seen from the rightmost vial in the inset of Figure 1, the stock solution of the as-prepared Ag nanoplates

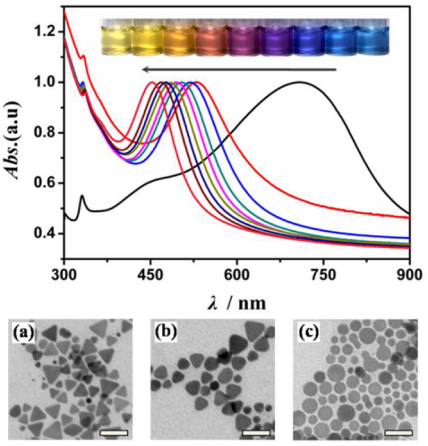

Figure 1. UV−vis−NIR extinction spectra of aqueous suspensions of Ag nanoplates before and after being stirred with GO for different time intervals at room temperature. The black spectrum represents the UV−vis−NIR extinction spectrum of the as-synthesized Ag nanoplate solution. The rest of the spectra from right to left represent suspensions of Ag nanoplates stirred with GO for 1, 3, 10, 20, 40, 70, 120, and 360 min, respectively. The inset at the top shows a digital photograph of the corresponding Ag nanoplate suspensions and Ag nanoplate/GO mixture solutions for different time intervals. (a−c) TEM images of (a) as-synthesized triangular Ag nanoplates, (b) Ag nanoplates after washing treatment, and (c) Ag nanoplates after being stirred with GO for 6 h. Scale bars are 50 nm.

exhibited a blue color, with its corresponding UV−vis−NIR spectrum displaying three distinct LSPR bands at 730, 460, and 331 nm, which are assigned to the in-plane dipole, in-plane quadrupole, and out-of-plane quadrupole plasmon resonances, respectively, of triangular nanoplates.[41] To remove most of the unreacted reagents, byproducts, and ligands, the as-prepared Ag nanoplate suspension was further centrifuged and washed with DI water before use. After three cycles of centrifugation, the in-plane dipole plasmon band of the Ag nanoplate suspension exhibited an obvious blue shift (Figure S1), indicating that the triangular structure of the Ag nanoplates had become less sharp after the process, as confirmed by the transmission electron microscopy (TEM) results shown in Figure 1a,b. This phenomenon, we believe, is mainly caused by the detachment of some ligands from the surface of the Ag nanoplates after the washing treatment, which makes the Ag nanoplates energetically unfavorable.[35] Furthermore, XPS was also used to further investigate the states of Ag. The XPS pattern of the resulting Ag nanoplates showed significant Ag 3d signals (Figure S2) for Ag $3d_{5/2}$ and $3d_{3/2}$ peaks at 368.23 and 374.21 eV, respectively, which indicates that Ag was mainly present in its metallic state.[42]

As reported previously,[35] Ag nanoplates can be complexed with GO nanosheets to modulate the shape transformation and, hence, the LSPR response (peak wavelength) of the resulting Ag nanoplates through the interaction between GO and the ligands on the surface of the Ag nanoplates. To complex Ag nanoplates with GO, adequate amount of purified GO were added to the Ag nanoplate solution under vigorous stirring. As shown in the inset of Figure 1, the color of the Ag nanoplate/GO mixture solution gradually changed from dark blue to purple, red, and finally yellow during 360 min. Meanwhile, the corresponding UV−vis−NIR spectra revealed that the in-plane dipole plasmon band of the nanoplates during the process was blue-shifted from 530 to 450 nm (Figure 1), which could be precisely modulated by simply controlling the stirring time. The shape of the silver nanoplates transformed to round during this process (Figure 1c), which is consistent with previous results.[35] In addition, as GO displays a maximum absorption peak centered at ∼230 nm and a shoulder peak at ∼300 nm (Figure S3) that can be assigned to the $\pi-\pi^*$ transition of aromatic C═C bonds and the $n-\pi^*$ transition of C═O bonds, respectively, the obvious enhancement of absorption in the range of 300−400 nm was caused by the addition of GO.

3.2. SERS Measurements of 4-ATP Using LSPR-Tunable Ag Nanoplate/GO as Substrates. As the SERS signal is highly sensitive to the LSPR properties of the nanoplasmonic substrate used,[43] we further exploited the LSPR tunability of the Ag nanoplate/GO system for SERS measurements. We first selected 4-ATP as a model target analyte and investigated its LSPR-dependent SERS performances. As a reference, Figure S4 presents the TEM image and Raman spectrum of the control GO sample. The Raman spectrum of GO presents two main characteristic peaks: the D band at ∼1350 cm^{-1} and the G band at ∼1596 cm^{-1}, arising from a breathing mode of *k*-point photons of A_{1g} symmetry and the first-order scattering of the E_{2g} phonon of sp^2 carbon atoms, respectively.[30,44]

Figure 2 shows the UV−vis−NIR extinction spectra of Ag nanoplate/GO mixtures after they had been stirred for different

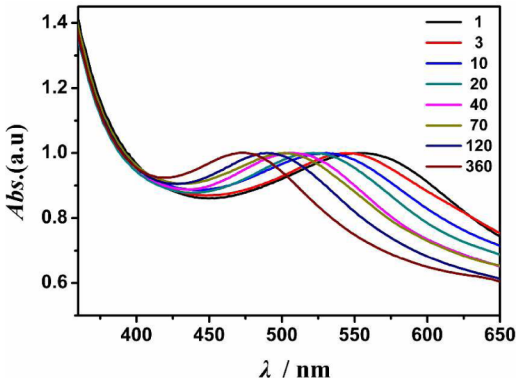

Figure 2. UV−vis−NIR extinction spectra of Ag nanoplate/GO complexes prepared by stirring for 1, 3, 10, 20, 40, 70, 120, and 360 min, as indicated, and modified with 4-ATP.

time intervals and modified with 4-ATP (10^{-7} M). Compared with that of pure Ag nanoplate/GO complexes, all of the UV−vis−NIR extinction spectra displayed a pronounced red shift (∼20 nm) of the LSPR band. The LSPR shift is indicative of the surface modification of the Ag nanoplate/GO complexes with 4-ATP by the change of the hydrogen-bond environment or the dielectric constant after the addition of 4-ATP.[45,46] In addition, we noticed that the out-of-plane quadrupole plasmon resonance of the Ag nanoplates became very weak after the GO complexation and 4-ATP modification. This is due to the gradual shape transformation of the Ag nanoplates (from triangular to round)[35,47] after three cycles of centrifugation (Figure 1b) and further complexing with GO and 4-ATP.

As seen from Figure 3a, the 4-ATP-modified Ag nanoplate/GO complexes presented different SERS spectra when they

DOI: 10.1021/acsami.5b04946
ACS Appl. Mater. Interfaces 2015, 7, 18038−18045

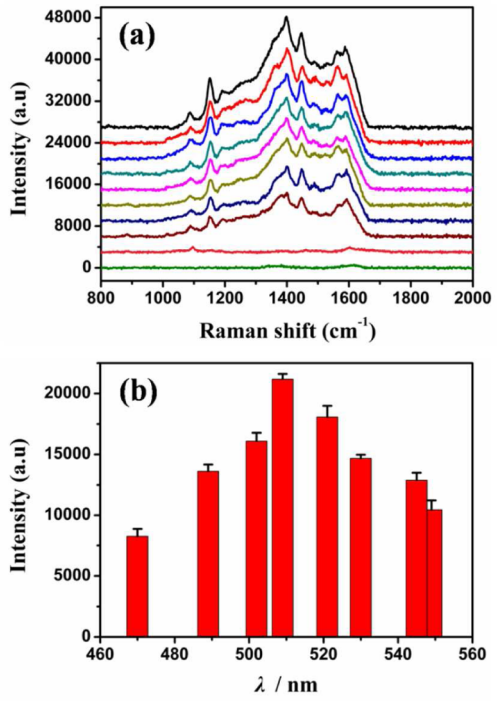

Figure 3. (a) Raman spectrum of pure 4-ATP (10^{-6} M, ninth line from the top) and pure Ag nanoplate/GO mixture (bottom line) and SERS spectra of 4-ATP (10^{-7} M) mixed with Ag nanoplate/GO mixtures and stirred for different time intervals (40, 20, 70, 10, 120, 3, 1, and 360 min, respectively, from the top to the eighth line). (b) Column diagram of the relationship between the UV−vis−NIR extinction peak and the SERS spectra (at ∼1394 cm^{-1}) of 4-ATP with the Ag nanoplate/GO complexes prepared by stirring for different time intervals (1, 3, 10, 20, 40, 70, 120, and 360 min, respectively, from right to left).

were stirred for different time intervals. There are five strong bands centered at about 1085, 1150, 1394, 1443, and 1565 cm^{-1} in the SERS spectra of the Ag nanoplate/GO/4-ATP system. As previously reported, the normal Raman spectrum of 4-ATP is mainly characterized by two strong bands at ∼1089 and ∼1595 cm^{-1},[8] which can be seen clearly in Figure 3a, even though the concentration of 4-ATP was very low. These obvious Raman spectrum differences are due to the occurrence of charge transfer from the Ag nanoplates to 4-ATP.[48] By comparing the Raman spectra of pure 4-ATP (10^{-6} M) and 4-ATP- (10^{-7} M) modified Ag nanoplate/GO complexes, two new strong Raman peaks can be observed for the latter at ∼1394 and ∼1443 cm^{-1}, which can be attributed to the N═N vibration of the *trans*-dimercaptoazobenzene (*trans*-DMAB) vibrational modes.[49] In addition, the pure Ag nanoplate/GO mixture presented only very weak Raman signal for GO. These results clearly demonstrated that the 4-ATP molecules were paired together to form the DMAB vibrational modes when they modified the Ag nanoplate surface.

Figure 3b shows a column diagram of the relationship between the UV−vis−NIR extinction spectra and the SERS spectra (∼1394 cm^{-1}) of Ag nanoplate/GO complexes prepared by stirring for different time intervals. The Ag nanoplate/GO complex prepared by stirring for 40 min displayed the largest SERS response. This is due to the greater overlap of the extinction peak (∼508 nm) of the Ag nanoplate/GO complex with the Raman excitation wavelength of the laser used (514.5 nm), causing the largest SERS response due to the LSPR effect. With the extinction peak of the resulting Ag nanoplate/GO complex deviating from the laser excitation wavelength, the SERS response of the system was subdued. The SERS spectrum detection was repeated at least three times for each sample to assess the reproducibility of the measurement.

3.3. SERS Measurements of 4-MBA Using LSPR-Tunable Ag Nanoplate/GO as Substrates. To test the wide applicability of Ag nanoplate/GO complexes, we selected 4-MBA as another target analyte and used a 785-nm diode laser, which is more suitable for 4-MBA signal detection for Raman excitation. Figure 4 shows the UV−vis−NIR extinction

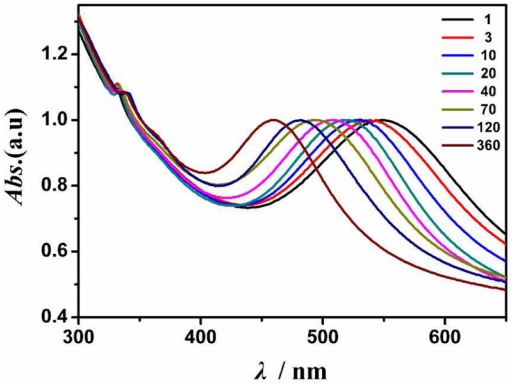

Figure 4. UV−vis−NIR extinction spectra of Ag nanoplate/GO complexes prepared by stirring for 1, 3, 10, 20, 40, 70, 120, and 360 min, as indicated, and modified with 4-MBA.

spectra of the 4-MBA-modified Ag nanoplate/GO complexes prepared by stirring for 1, 3, 10, 20, 40, 70, 120, and 360 min. As can be seen in Figure 4, the UV−vis−NIR extinction spectra of the Ag nanoplate/GO complexes after the addition of 4-MBA also displayed a red shift (∼22 nm) compared with that of a 4-MBA-free Ag nanoplate/GO mixture.

Figure 5a shows typical Raman spectra of pure 4-MBA (10^{-6} M) and a pure Ag nanoplate/GO mixture and the SERS spectra of 4-MBA (10^{-7} M) with Ag nanoplate/GO complexes prepared by stirring for different time intervals. From the top to the bottom are the SERS spectra of 4-MBA in the presence of Ag nanoplate/GO complexes prepared by stirring for 1, 3, 10, 20, 40, 70, 120, and 360 min and the Raman spectra of free 4-MBA and pure Ag nanoplate/GO mixture, respectively. As can be seen from Figure 5a, the pure 4-MBA (10^{-6} M) and Ag nanoplate/GO mixture exhibited no obvious Raman signals. The SERS spectra of 4-MBA with Ag nanoplate/GO complexes are dominated by the ν_{8a} (∼1590 cm^{-1}) and ν_{12} (∼1080 cm^{-1}) aromatic ring vibrations; other weak bands at ∼1150 and ∼1180 cm^{-1} are attributed to C—H deformation modes.[50] Figure 5b shows a column diagram of the relationship between the UV−vis−NIR extinction spectra and the SERS spectra (at 1080 cm^{-1}) of the Ag nanoplate/GO complexes prepared by stirring for different time intervals. As can be seen from Figure 5b, with the LSPR peak of the resulting Ag nanoplate/GO complexes approaching the excitation wavelength of the laser used, the SERS spectra of 4-MBA increased gradually due to the LSPR effect.

Although GO-supported Ag nanoplates prepared by stirring for different time intervals all showed SERS enhancement, it was clear that their SERS activities were quite different. To evaluate the enhancement effect of a SERS-active substrate, the enhancement factor (EF) is usually used.[51,52] Because an

DOI: 10.1021/acsami.5b04946
ACS Appl. Mater. Interfaces 2015, 7, 18038−18045

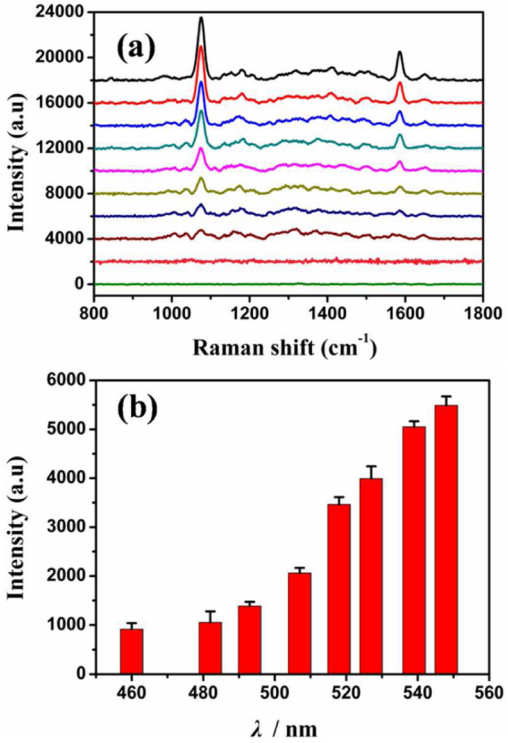

Figure 5. (a) Raman spectra of pure 4-MBA (10^{-6} M, ninth line from the top) and pure Ag nanoplate/GO mixture (bottom line) and SERS spectra of 4-MBA (10^{-7} M) mixed with Ag nanoplate/GO complexes and stirred for different time intervals (1, 3, 10, 20, 40, 70, 120, and 360 min, respectively, from the top to the eighth line). (b) Column diagram of the relationship between the UV−vis−NIR extinction spectra and the SERS spectrum (at 1080 cm^{-1}) of 4-MBA with the Ag nanoplate/GO complexes prepared by stirring for different time intervals (1, 3, 10, 20, 40, 70, 120, and 360 min, respectively, from right to left).

accurate volume and surface area of the Ag nanoplates at each stage are difficult to obtain, it is hard to calculate reliable EFs for Ag nanoplates with evolving/different morphologies. Therefore, the apparent enhancement factor (AEF) was selected to represent the SERS activity of the GO-supported Ag nanoplates. Based on a previous report,[53] AgNPs were chosen as a reference for calculating the AEF of GO-supported Ag nanoplates. Figure S5 presents the TEM image and UV−vis−NIR extinction spectra of the control AgNPs. The AEF of the GO/Ag nanoplate complexes was defined as AEF = $(I_{SERS}/I_0)(C_0/C_{SERS})$. For the 4-ATP-modified Ag nanoplate/GO complexes, I_{SERS} is the intensity of the peak at 1150 cm^{-1} in the SERS spectrum; I_0 is the intensity of the same peak in the SERS spectrum on AgNPs (Figure S6A); and C_{SERS} and C_0 refer to the concentrations of 4-ATP in Ag nanoplate/GO complexes (10^{-7} M) and AgNP colloids (10^{-3} M), respectively.[53,54] For the 4-MBA-modified Ag nanoplate/GO complexes, I_{SERS} is the intensity of the peak at 1080 cm^{-1} in the SERS spectrum; I_0 is the intensity of the same peak in the SERS spectrum on AgNPs (Figure S6B); and C_{SERS} and C_0 refer to the concentrations of 4-MBA in Ag nanoplate/GO complexes (10^{-7} M) and AgNP colloids (10^{-3} M), respectively. Taking into account the fact that the SERS signal on the Ag nanoplate/GO complexes is derived from 4-ATP with a concentration diluted by a factor of 10^4 as compared with that used in AgNPs at the same accumulation times and laser power, the AEF for Ag nanoplate/GO complexes relative to AgNP colloid was calculated to be on the order of 10^4, as shown in Table 1. Although the AEF values cannot elucidate the real EF for the Ag nanoplate/GO complexes, they do demonstrate that the SERS enhancement of the Ag nanoplate/GO complexes is 10^4 times larger than that from the commonly used AgNPs, which is comparable to or even better than those of other reported SERS-active substrates.[43,54] This is because graphene nanosheets also represent an excellent SERS substrate for the adsorption of some metal nanoparticles, which can effectively induce the electron-transfer ability as well as a large EE effect between graphene and the molecules adsorbed on its surface.[30] Therefore, SERS enhancement using GO-supported Ag nanoplates would benefit from the EE effect among the graphene nanosheets, Ag nanoplates, and adsorbed analytes.

Table 1. SERS Apparent Enhancement Factors of GO-Supported Ag Nanoplates[a] Calculated Based on the Peak at 1150 cm^{-1} in the SERS Spectrum of 4-ATP and the Peak at 1080 cm^{-1} in the SERS Spectrum of 4-MBA Excited at 514 and 785 nm, Respectively

time (min)	4-ATP	4-MBA
1	4.2×10^4	6.6×10^4
3	4.9×10^4	6.1×10^4
10	6.4×10^4	4.8×10^4
20	7.9×10^4	4.2×10^4
40	1.0×10^5	2.5×10^4
70	6.6×10^4	1.7×10^4
120	6.0×10^4	1.3×10^4
360	3.5×10^4	1.1×10^4

[a]Relative to AgNP colloid.

Table 1 clearly shows the tendency of the AEF to change with the LSPR wavelength of the substrate used. In the case of 4-ATP detection (with an excitation wavelength of 514 nm), a 1-order-of-magnitude-larger SERS AEF was obtained using the GO-supported Ag nanoplates prepared by stirring for 40 min than using the other samples with LSPR peaks shifted gradually away from the 514-nm excitation laser wavelength. Similarly, in the case of 4-MBA detection (with an excitation wavelength of 785 nm), the SERS intensity dropped off gradually as the LSPR band of the resulting substrate blue-shifted (away from the 785-nm excitation laser wavelength). The results clearly show a dependency of the AEF on the overlap of the Raman excitation wavelength and the LSPR peak of the substrate. The Raman signals were greatly enhanced when the laser excitation line matched the LSPR band of the substrate used. In this way, the excitation of LSPR generated a significantly enhanced electromagnetic field at the surface of the nanostructure and hence enhanced the SERS signals.

3.4. Relationship between the SERS Response and the Concentration of Target Analyte. Impressively, when the GO-supported Ag nanoplates were applied for the SERS detection of 4-MBA, the sensitivity was extremely high. Figure 6A displays the SERS spectra of GO-supported Ag nanoplates with different concentrations of 4-MBA. Obviously, the SERS spectra of GO-supported Ag nanoplates increased as the 4-MBA concentration was increased from 10^{-12} to 10^{-7} M. Figure 6B shows the calibration curve for the SERS spectra of GO-supported Ag nanoplates (at 1080 cm^{-1}) as a function of the logarithm of 4-MBA concentration. A linear response range of 4-MBA was found from 10^{-12} to 10^{-7} M, with a correlation coefficient of 0.990. The linear progress equation was Y =

DOI: 10.1021/acsami.5b04946
ACS Appl. Mater. Interfaces 2015, 7, 18038−18045

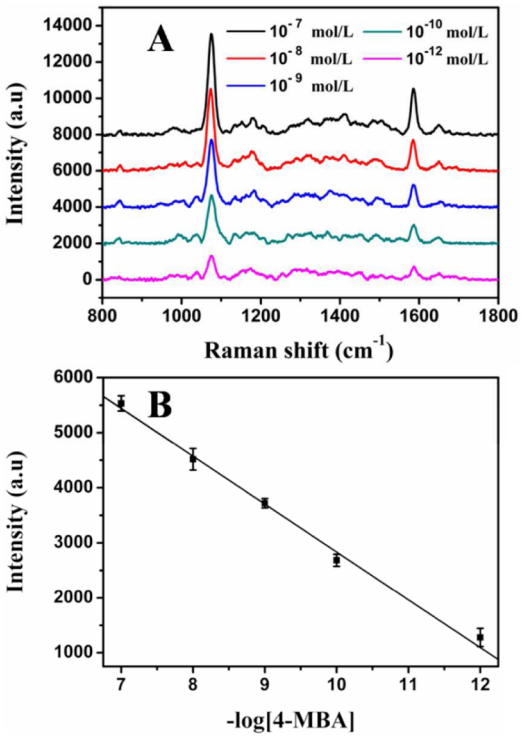

Figure 6. (A) SERS spectra of GO-supported Ag nanoplates with different concentrations of 4-MBA. (B) Corresponding calibration curve of SERS intensity versus −log [4-MBA], in which the SERS intensities were recorded at 1080 cm^{-1}.

11528.7 − 869.45*X*, where *Y* is the Raman intensity and *X* is the logarithm of the 4-MBA concentration. Based on a signal-to-noise ratio of 5,[55] the theoretical 4-MBA limit of detection (LOD) of 5×10^{-14} M was deduced from the linear regression equation.[30]

3.5. SERS Reproducibility and Stability of GO-Supported Ag Nanoplates. For an excellent SERS-active nanomaterial, high reproducibility and stability are critical for practical use. To investigate the reproducibility of the GO-supported Ag nanoplates as substrates for SERS applications, six samples modified with 4-ATP and 4-MBA were chosen randomly. As shown in Figure 7, SERS spectra of the 4-ATP- and 4-MBA-modified GO-supported Ag nanoplates samples prepared by stirring for 20 and 1 min , respectively, presented highly reproducible Raman signals. The SERS reproducibility and stability of the GO-supported Ag nanoplates were also tested quantitatively. The SERS reproducibility of the GO-supported Ag nanoplates for 4-ATP and 4-MBA was achieved with variations of less than 10%, and the substrate could be retained for at least 1 month without any obvious change in SERS signals. Therefore, the results indicated good SERS reproducibility and stability of the GO-supported Ag nanoplate substrate for SERS applications.

4. CONCLUSIONS

In conclusion, we have demonstrated a SERS platform with high sensitivity based on silver nanoplates that can modulate their LSPR responses through simple control of the stirring time with GO. The Raman spectra of 4-MBA and 4-ATP using the Ag nanoplate/GO complexes as substrates were selected and tested in this study. GO-supported Ag nanoplates having an LSPR peak closest to the Raman excitation laser wavelength showed the strongest SERS responses. The SERS enhancement factor of the Ag nanoplate/GO complexes was ~10^4 times larger than that obtained using spherical AgNPs, which is comparable to or even better than those of other reported SERS-active substrates. The Ag nanoplate/GO complexes were also used to detect 4-MBA and 4-ATP with high sensitivity and reproducibility. In addition, the as-obtained GO-supported Ag nanoplates exhibited excellent stability over a long time without any noticeable changes in their optical properties and SERS responses. We believe that the ease of obtaining Ag nanoplates with tunable LSPR responses and excellent reproducibility and stability should be beneficial not only for practical SERS applications but also for biosensing, multicolor diagnostic labeling, and so on.

■ ASSOCIATED CONTENT

Supporting Information

The Supporting Information is available free of charge on the ACS Publications website at DOI: 10.1021/acsami.5b04946.

UV−vis−NIR extinction spectra of GO, AgNPs, and Ag nanoplates after three cycles of centrifugation; XPS spectra of Ag nanoplates; Raman spectra of GO nanosheets and AgNPs modified with 4-ATP and 4-MBA as model target analytes; and TEM images of GO nanosheets and AgNPs (PDF)

■ AUTHOR INFORMATION

Corresponding Author

*E-mail: ydjin@ciac.ac.cn. Tel.: +86-431-85262661. Fax: +86-431-85262661.

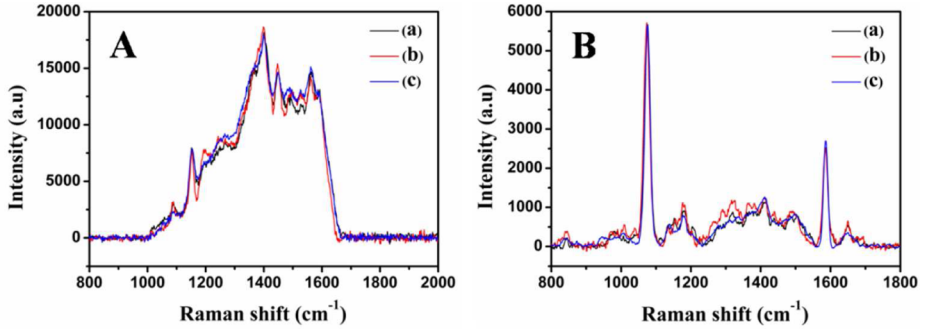

Figure 7. (A) SERS spectra of three independent GO-supported Ag nanoplate samples prepared by stirring for 20 min and absorbed with 4-ATP. (B) SERS spectra of three independent GO-supported Ag nanoplates prepared by stirring for 1 min and absorbed with 4-MBA.

DOI: 10.1021/acsami.5b04946
ACS Appl. Mater. Interfaces 2015, 7, 18038−18045

Author Contributions

The manuscript was written through contributions of all authors. All authors have given approval to the final version of the manuscript.

Notes

The authors declare no competing financial interest.

■ ACKNOWLEDGMENTS

This work was supported by the National Science Foundation of China (Nos. 21475125, 21175125), the Hundred Talents Program of the Chinese Academy of Sciences, and the State Key Laboratory of Electroanalytical Chemistry (No. 110000R387).

■ REFERENCES

(1) Jeanmaire, D. L.; Van Duyne, R. P. Surface Raman Spectroelectrochemistry: Part I. Heterocyclic, Aromatic, and Aliphatic Amines Adsorbed on the Anodized Silver Electrode. *J. Electroanal. Chem. Interfacial Electrochem.* **1977**, *84*, 1−20.

(2) Fleischmann, M.; Hendra, P. J.; McQuillan, A. J. Raman Spectra from Electrode Surfaces. *J. Chem. Soc., Chem. Commun.* **1973**, *3*, 80−81.

(3) Kubackova, J.; Fabriciova, G.; Miskovsky, P.; Jancura, D.; Sanchez-Cortes, S. Sensitive Surface-Enhanced Raman Spectroscopy (SERS) Detection of Organochlorine Pesticides by Alkyl Dithiol-Functionalized Metal Nanoparticles-Induced Plasmonic Hot Spots. *Anal. Chem.* **2015**, *87*, 663−669.

(4) Lee, S. J.; Morrill, A. R.; Moskovits, M. Hot Spots in Silver Nanowire Bundles for Surface-Enhanced Raman Spectroscopy. *J. Am. Chem. Soc.* **2006**, *128*, 2200−2201.

(5) Orendorff, C. J.; Gole, A.; Sau, T. K.; Murphy, C. J. Surface-Enhanced Raman Spectroscopy of Self-Assembled Monolayers: Sandwich Architecture and Nanoparticle Shape Dependence. *Anal. Chem.* **2005**, *77*, 3261−3266.

(6) Zhang, J.; Gao, Y.; Alvarez-Puebla, R. A.; Buriak, J. M.; Fenniri, H. Synthesis and SERS Properties of Nanocrystalline Gold Octahedra Generated from Thermal Decomposition of $HAuCl_4$ in Block Copolymers. *Adv. Mater.* **2006**, *18*, 3233−3237.

(7) Braun, G.; Lee, S. J.; Dante, M.; Nguyen, T.-Q.; Moskovits, M.; Reich, N. Surface-Enhanced Raman Spectroscopy for DNA Detection by Nanoparticle Assembly onto Smooth Metal Films. *J. Am. Chem. Soc.* **2007**, *129*, 6378−6379.

(8) Zhang, Z.; Xu, F.; Yang, W.; Guo, M.; Wang, X.; Zhang, B.; Tang, J. A Facile One-Pot Method to High-Quality Ag-Graphene Composite Nanosheets for Efficient Surface-Enhanced Raman Scattering. *Chem. Commun.* **2011**, *47*, 6440−6442.

(9) Jiang, J.; Bosnick, K.; Maillard, M.; Brus, L. Single Molecule Raman Spectroscopy at the Junctions of Large Ag Nanocrystals. *J. Phys. Chem. B* **2003**, *107*, 9964−9972.

(10) Tao, A.; Kim, F.; Hess, C.; Goldberger, J.; He, R.; Sun, Y.; Xia, Y.; Yang, P. Langmuir−Blodgett Silver Nanowire Monolayers for Molecular Sensing Using Surface-Enhanced Raman Spectroscopy. *Nano Lett.* **2003**, *3*, 1229−1233.

(11) Liu, G.; Cai, W.; Kong, L.; Duan, G.; Li, Y.; Wang, J.; Cheng, Z. Trace Detection of Cyanide Based on SERS Effect of Ag Nanoplate-Built Hollow Microsphere Arrays. *J. Hazard. Mater.* **2013**, *248*−*249*, 435−441.

(12) Kneipp, K.; Kneipp, H.; Itzkan, I.; Dasari, R. R.; Feld, M. S. Ultrasensitive Chemical Analysis by Raman Spectroscopy. *Chem. Rev.* **1999**, *99*, 2957−2976.

(13) Pavel, I.; McCarney, E.; Elkhaled, A.; Morrill, A.; Plaxco, K.; Moskovits, M. Label-Free SERS Detection of Small Proteins Modified to Act as Bifunctional Linkers. *J. Phys. Chem. C* **2008**, *112*, 4880−4883.

(14) Zhao, X.; Hosmane, N. S.; Wu, A. ortho-Phenylenediamine: An Effective Spacer to Build Highly Magnetic Fe_3O_4/Au Nanocomposites. *ChemPhysChem* **2012**, *13*, 4142−4147.

(15) Shen, A.; Chen, L.; Xie, W.; Hu, J.; Zeng, A.; Richards, R.; Hu, J. Triplex Au−Ag−C Core−Shell Nanoparticles as a Novel Raman Label. *Adv. Funct. Mater.* **2010**, *20*, 969−975.

(16) Cao, Y. C.; Jin, R.; Mirkin, C. A. Nanoparticles with Raman Spectroscopic Fingerprints for DNA and RNA Detection. *Science* **2002**, *297*, 1536−1540.

(17) Tebbe, M.; Kuttner, C.; Männel, M.; Fery, A.; Chanana, M. Colloidally Stable and Surfactant-Free Protein-Coated Gold Nanorods in Biological Media. *ACS Appl. Mater. Interfaces* **2015**, *7*, 5984−5991.

(18) Cao, Y. C.; Jin, R.; Nam, J.-M.; Thaxton, C. S.; Mirkin, C. A. Raman Dye-Labeled Nanoparticle Probes for Proteins. *J. Am. Chem. Soc.* **2003**, *125*, 14676−14677.

(19) Arenas, J. F.; Woolley, M. S.; Tocón, I. L.; Otero, J. C.; Marcos, J. I. Complete Analysis of the Surface-Enhanced Raman Scattering of Pyrazine on the Silver Tlectrode on the Basis of a Resonant Charge Transfer Mechanism Involving Three States. *J. Chem. Phys.* **2000**, *112*, 7669−7683.

(20) Wu, X.; Luo, L.; Yang, S.; Ma, X.; Li, Y.; Dong, C.; Tian, Y.; Zhang, L. e.; Shen, Z.; Wu, A. Improved SERS Nanoparticles for Direct Detection of Circulating Tumor Cells in the Blood. *ACS Appl. Mater. Interfaces* **2015**, *7*, 9965−9971.

(21) Penn, M. A.; Drake, D. M.; Driskell, J. D. Accelerated Surface-Enhanced Raman Spectroscopy (SERS)-Based Immunoassay on a Gold-Plated Membrane. *Anal. Chem.* **2013**, *85*, 8609−8617.

(22) Cui, Q.; Shen, G.; Yan, X.; Li, L.; Möhwald, H.; Bargheer, M. Fabrication of Au@Pt Multibranched Nanoparticles and Their Application to In Situ SERS Monitoring. *ACS Appl. Mater. Interfaces* **2014**, *6*, 17075−17081.

(23) Leopold, N.; Lendl, B. A New Method for Fast Preparation of Highly Surface-Enhanced Raman Scattering (SERS) Active Silver Colloids at Room Temperature by Reduction of Silver Nitrate with Hydroxylamine Hydrochloride. *J. Phys. Chem. B* **2003**, *107*, 5723−5727.

(24) Zhang, L.; Wang, B.; Zhu, G.; Zhou, X. Synthesis of Silver Nanowires as a SERS Substrate for the Detection of Pesticide Thiram. *Spectrochim. Acta, Part A* **2014**, *133*, 411−416.

(25) Zhang, L. Self-Assembly Ag Nanoparticle Monolayer Film as SERS Substrate for Pesticide Detection. *Appl. Surf. Sci.* **2013**, *270*, 292−294.

(26) Zhang, W.; Li, B.; Chen, L.; Wang, Y.; Gao, D.; Ma, X.; Wu, A. Brushing, a Simple Way to Fabricate SERS Active Paper Substrates. *Anal. Methods* **2014**, *6*, 2066−2071.

(27) Willets, K. A.; Van Duyne, R. P. Localized Surface Plasmon Resonance Spectroscopy and Sensing. *Annu. Rev. Phys. Chem.* **2007**, *58*, 267−297.

(28) Tian, Z.-Q.; Ren, B.; Wu, D.-Y. Surface-Enhanced Raman Scattering: From Noble to Transition Metals and from Rough Surfaces to Ordered Nanostructures. *J. Phys. Chem. B* **2002**, *106*, 9463−9483.

(29) Xu, C.; Wang, X. Fabrication of Flexible Metal-Nanoparticle Films Using Graphene Oxide Sheets as Substrates. *Small* **2009**, *5*, 2212−2217.

(30) Liu, M.; Chen, W. Graphene Nanosheets-Supported Ag Nanoparticles for Ultrasensitive Detection of TNT by Surface-Enhanced Raman Spectroscopy. *Biosens. Bioelectron.* **2013**, *46*, 68−73.

(31) He, P.; Liu, H.; Li, Z.; Liu, Y.; Xu, X.; Li, J. Electrochemical Deposition of Silver in Room-Temperature Ionic Liquids and Its Surface-Enhanced Raman Scattering Effect. *Langmuir* **2004**, *20*, 10260−10267.

(32) Wang, L.; Li, H.; Tian, J.; Sun, X. Monodisperse, Micrometer-Scale, Highly Crystalline, Nanotextured Ag Dendrites: Rapid, Large-Scale, Wet-Chemical Synthesis and their Application as SERS Substrates. *ACS Appl. Mater. Interfaces* **2010**, *2*, 2987−2991.

(33) Neddersen, J.; Chumanov, G.; Cotton, T. M. Laser Ablation of Metals: A New Method for Preparing SERS Active Colloids. *Appl. Spectrosc.* **1993**, *47*, 1959−1964.

(34) Ren, W.; Fang, Y.; Wang, E. A Binary Functional Substrate for Enrichment and Ultrasensitive SERS Spectroscopic Detection of Folic Acid Using Graphene Oxide/Ag Nanoparticle Hybrids. *ACS Nano* **2011**, *5*, 6425−6433.

DOI: 10.1021/acsami.5b04946
ACS Appl. Mater. Interfaces 2015, 7, 18038−18045

(35) Wang, P.; He, H.; Jin, Y. Shape Transformation and Visible Region Plasmonic Modulation of Silver Nanoplates by Graphene Oxide. *Small* **2012**, *8*, 3438−3442.
(36) Xu, W.; Ling, X.; Xiao, J.; Dresselhaus, M. S.; Kong, J.; Xu, H.; Liu, Z.; Zhang, J. Surface Enhanced Raman Spectroscopy on a Flat Graphene Surface. *Proc. Natl. Acad. Sci. U. S. A.* **2012**, *109*, 9281−9286.
(37) Hummers, W. S.; Offeman, R. E. Preparation of Graphitic Oxide. *J. Am. Chem. Soc.* **1958**, *80*, 1339−1339.
(38) Zhang, Q.; Li, N.; Goebl, J.; Lu, Z.; Yin, Y. A Systematic Study of the Synthesis of Silver Nanoplates: Is Citrate a "Magic" Reagent? *J. Am. Chem. Soc.* **2011**, *133*, 18931−18939.
(39) Métraux, G. S.; Mirkin, C. A. Rapid Thermal Synthesis of Silver Nanoprisms with Chemically Tailorable Thickness. *Adv. Mater.* **2005**, *17*, 412−415.
(40) Guo, S.; Dong, S.; Wang, E. A General Method for the Rapid Synthesis of Hollow Metallic or Bimetallic Nanoelectrocatalysts with Urchinlike Morphology. *Chem. - Eur. J.* **2008**, *14*, 4689−4695.
(41) Tang, B.; Xu, S.; An, J.; Zhao, B.; Xu, W. Photoinduced Shape Conversion and Reconstruction of Silver Nanoprisms. *J. Phys. Chem. C* **2009**, *113*, 7025−7030.
(42) Liu, M.; Lu, Y.; Chen, W. PdAg Nanorings Supported on Graphene Nanosheets: Highly Methanol-Tolerant Cathode Electrocatalyst for Alkaline Fuel Cells. *Adv. Funct. Mater.* **2013**, *23*, 1289−1296.
(43) Tan, T.; Tian, C.; Ren, Z.; Yang, J.; Chen, Y.; Sun, L.; Li, Z.; Wu, A.; Yin, J.; Fu, H. LSPR-dependent SERS Performance of Silver Nanoplates with Highly Stable and Broad Tunable LSPRs Prepared Through an Improved Seed-Mediated Strategy. *Phys. Chem. Chem. Phys.* **2013**, *15*, 21034−21042.
(44) Lu, Y.; Jiang, Y.; Wei, W.; Wu, H.; Liu, M.; Niu, L.; Chen, W. Novel Blue Light Emitting Graphene Oxide Nanosheets Fabricated by Surface Functionalization. *J. Mater. Chem.* **2012**, *22*, 2929−2934.
(45) Li, X.; Liu, L.; Schlegel, H. B. On the Physical Origin of Blue-Shifted Hydrogen Bonds. *J. Am. Chem. Soc.* **2002**, *124*, 9639−9647.
(46) Yang, Y.; Zhang, W.; Pei, S.; Shao, J.; Huang, W.; Gao, X. Blue-Shifted and Red-Shifted Hydrogen Bonds: Theoretical Study of the $CH_3CHO\cdots NH_3$ Complexes. *J. Mol. Struct.: THEOCHEM* **2005**, *732*, 33−37.
(47) Kelly, K. L.; Coronado, E.; Zhao, L. L.; Schatz, G. C. The Optical Properties of Metal Nanoparticles: The Influence of Size, Shape, and Dielectric Environment. *J. Phys. Chem. B* **2003**, *107*, 668−677.
(48) Osawa, M.; Matsuda, N.; Yoshii, K.; Uchida, I. Charge Transfer Resonance Raman Process in Surface-Enhanced Raman Scattering from P-Aminothiophenol Adsorbed on Silver: Herzberg-Teller Contribution. *J. Phys. Chem.* **1994**, *98*, 12702−12707.
(49) Fang, Y.; Li, Y.; Xu, H.; Sun, M. Ascertaining p,p′-Dimercaptoazobenzene Produced from p-Aminothiophenol by Selective Catalytic Coupling Reaction on Silver Nanoparticles. *Langmuir* **2010**, *26*, 7737−7746.
(50) Li, S.; Xu, P.; Ren, Z.; Zhang, B.; Du, Y.; Han, X.; Mack, N. H.; Wang, H.-L. Fabrication of Thorny Au Nanostructures on Polyaniline Surfaces for Sensitive Surface-Enhanced Raman Spectroscopy. *ACS Appl. Mater. Interfaces* **2013**, *5*, 49−54.
(51) Zuo, Z.; Zhu, K.; Ning, L.; Cui, G.; Qu, J.; Cheng, Y.; Wang, J.; Shi, Y.; Xu, D.; Xin, Y. Highly Sensitive Surface Enhanced Raman Scattering Substrates Based on Ag Decorated Si Nanocone Arrays and their Application in Trace Dimethyl Phthalate Detection. *Appl. Surf. Sci.* **2015**, *325*, 45−51.
(52) Fang, H.; Zhang, C. X.; Liu, L.; Zhao, Y. M.; Xu, H. J. Recyclable Three-Dimensional Ag Nanoparticle-Decorated TiO_2 Nanorod Arrays for Surface-Enhanced Raman Scattering. *Biosens. Bioelectron.* **2015**, *64*, 434−441.
(53) Ren, W.; Guo, S.; Dong, S.; Wang, E. A Simple Route for the Synthesis of Morphology-Controlled and SERS-Active Ag Dendrites with Near-Infrared Absorption. *J. Phys. Chem. C* **2011**, *115*, 10315−10320.
(54) Wang, Y.; Chen, H.; Dong, S.; Wang, E. Fabrication and Characterization of SERS-active Silver Clusters on Glassy Carbon. *J. Raman Spectrosc.* **2007**, *38*, 515−521.
(55) Riskin, M.; Tel-Vered, R.; Lioubashevski, O.; Willner, I. Ultrasensitive Surface Plasmon Resonance Detection of Trinitrotoluene by a Bis-aniline-Cross-Linked Au Nanoparticles Composite. *J. Am. Chem. Soc.* **2009**, *131*, 7368−7378.

DOI: 10.1021/acsami.5b04946
ACS Appl. Mater. Interfaces 2015, 7, 18038−18045